



**HAL**  
open science

# A parametric analysis of the effect of the jet initial conditions on the wavelet-decomposed near-field acoustic pressure

Stefano Meloni, Roberto Camussi, Matteo Mancinelli, Christophe Bogey

► **To cite this version:**

Stefano Meloni, Roberto Camussi, Matteo Mancinelli, Christophe Bogey. A parametric analysis of the effect of the jet initial conditions on the wavelet-decomposed near-field acoustic pressure. 29th AIAA/CEAS Aeroacoustics Conference, Jun 2023, San Diego, CA, United States. pp.4289, 10.2514/6.2023-4289 . hal-04122927

**HAL Id: hal-04122927**

**<https://hal.science/hal-04122927>**

Submitted on 16 Jun 2023

**HAL** is a multi-disciplinary open access archive for the deposit and dissemination of scientific research documents, whether they are published or not. The documents may come from teaching and research institutions in France or abroad, or from public or private research centers.

L'archive ouverte pluridisciplinaire **HAL**, est destinée au dépôt et à la diffusion de documents scientifiques de niveau recherche, publiés ou non, émanant des établissements d'enseignement et de recherche français ou étrangers, des laboratoires publics ou privés.

# A parametric analysis of the effect of the jet initial conditions on the wavelet-decomposed near-field acoustic pressure

S. Meloni\*

*Università della Tuscia, Viterbo, Italy*

R. Camussi<sup>†</sup>, M. Mancinelli<sup>‡</sup>

*Università degli Studi Roma Tre, Rome, Italy*

C. Bogey<sup>§</sup>

*Univ Lyon, CNRS, Ecole Centrale de Lyon, INSA Lyon, Université Claude Bernard Lyon I, Ecully, France*

**This paper reports a parametric analysis of the effect of the different nozzle exhaust initial conditions on the acoustic pressure generated by a single stream cold jet in its near field. The study has been performed by processing a numerical database obtained by large-eddy simulations of jet flows at  $M=0.9$  and  $Re=10^5$ , characterized by different nozzle exhaust turbulence intensities and boundary layer thicknesses. Pressure signals have been recorded by virtual probes distributed in several radial and axial positions in the near field of the jet covering up to  $20D$  in the streamwise direction and  $6D$  in the radial, and the acoustic component is extracted using a wavelet-based tool. The reconstructed acoustic time series are then analyzed both in the time and frequency domains. The results show that the boundary-layer thickness and the turbulence level significantly affect the acoustic pressure in terms of its intensity and directivity. The sideline directivity is observed to decrease for increasing turbulence level whereas it increases with the boundary layer thickness. The streamwise directivity has the opposite trend probably as an effect of the large scale. Also the energy distribution in the frequency domain depends appreciably on the aforementioned parameters but only at axial distances smaller than about  $10D$ .**

## I. Introduction

The high-speed flow issuing from the jet exhaust of the propulsive system of modern civil aircraft is known to be one of the main sources of noise during take-off. Since the seminal work of Lighthill[1], many studies have been devoted to identifying the physical mechanisms by which jet turbulent structures generate noise (see e.g. [2–4]). To the extent of physical understanding and modelling, a significant progress has been accomplished recently by the use of a wavepacket source model and by the application of linear stability analysis (see among many [5–7]). However, despite the indisputable success of these approaches, several aspects still remain unclear and need further investigations.

One of the open questions, that is the subject of the present analysis, concerns the influence of the conditions of the flow at the jet exit on the generation of acoustic waves and on their propagation towards the far field. Indeed, according to the literature [8–11], the flow state at the nozzle exhaust plays a key role in the noise emission since it influences relevant physical mechanisms correlated to jet noise generation, such as the laminar-to-turbulent transition of the near wall flow and the flow mixing in the jet plume [12].

Several studies in literature have shown that, in addition to the Reynolds ( $Re$ ) and Mach number ( $M$ ), the main jet-exit flow properties that can be directly correlated to the acoustic emissions are the shear layer momentum thickness, the boundary layer (BL) velocity profile and the turbulence intensity ( $TI$ ). These parameters are difficult to be varied and controlled in experiments and may vary unexpectedly from one experiment to another even when  $Re$  and  $M$  are supposed to be the same. Thus, the only way to evaluate quantitatively their efficacy in influencing jet noise is through numerical simulations and this motivated the relevant effort pursued in this field during the last decades [10, 11, 13–16].

---

\*Assistant Professor, Department of Economics, Engineering, Society and Business Organization, 01100 Viterbo, Italy, stefano.meloni@unitus.it, AIAA member

<sup>†</sup>Full Professor, Department of Engineering, Via della Vasca Navale 79, 00146 Rome, Italy, roberto.camussi@uniroma3.it, AIAA member

<sup>‡</sup>Assistant Professor, Department of Engineering, Via della Vasca Navale 79, 00146 Rome, Italy, matteo.mancinelli@uniroma3.it, AIAA member

<sup>§</sup>CNRS Research Director, Laboratoire de Mécanique des Fluides et d'Acoustique, UMR 5509, Ecully, France, christophe.bogey@ec-lyon.fr, AIAA Associate Fellow

The present study aims at complementing these literature outcomes by analyzing in details an extensive numerical database covering several flow conditions at the nozzle exit of a compressible subsonic jet.

The parametric analysis proposed therein attempts to clarify the sensitivity of the acoustic pressure in the near-field upon the initial conditions. Indeed, the investigation is focused on the region close to the jet flow where, as pointed out in [17], the beginnings of sound, destined to become noise in the far field, are contained.

The present investigation is based on the post-processing of a huge large-eddy-simulation (LES) database containing pressure time series covering a domain that varies in the stream-wise direction from  $x=0$  up to  $x/D=20$  and in the radial direction from  $r/D=0.5$  (nozzle line) up to  $r/D=3$ , where  $D$  is the jet exit diameter. Simulations have been performed by varying the nozzle exhaust turbulence intensity from  $TI = 0\%$ , which corresponds to a fully laminar case, up to  $TI = 15\%$ , which is representative of a fully disturbed jet, with a step of  $\Delta TI$  of 3%. The second parameter explored is the boundary layer thickness  $\delta_{BL}$ , normalized by the nozzle exhaust radius  $r_0$ . Specifically, the value of  $\delta_{BL}/r_0$  spans from 0.025 up to 0.4, doubling the value of the thickness at each step, and keeping fixed the nozzle exhaust turbulence intensity at  $TI = 0\%$ .

It is known that (see e.g. [17–22]) the near-field pressure contains a propagating acoustic part and a non-propagating hydrodynamic (or pseudo-sound) counterpart, whence the exigence to analyse the two pressure components separately. In this work, the acoustic component of the pressure time series is extracted by applying a procedure well assessed in the literature [21] and based on the application of wavelet transform to the pressure data. The decomposed signals are then analyzed separately in terms of statistical quantities in the physical and Fourier domains.

Further details on the numerical setup and the wavelet-based processing procedure are given in Sections 2 and 3 respectively. Main results are reported in Sec. 4 whereas conclusions and final remarks are given in Sec.5.

## II. Numerical setup

Large Eddy Simulations of round free jets at a Reynolds number  $Re = 10^5$  and  $M=0.9$  have been used for the analysis reported in this paper. The first set of LES considers jets with a nozzle exhaust boundary layer thickness fixed at  $\delta_{BL} = 0.15r_0$ . The nozzle exit turbulence intensity has been varied in all the different simulations with a step of  $\Delta TI = 3\%$ , starting from a fully laminar case with  $TI = 0\%$  to the fully disturbed case  $TI = 15\%$ . These conditions have been achieved by tripping the pipe boundary layers and using random low-level vortical disturbances decorrelated in the azimuthal direction. A second set of simulations has been carried out with  $TI = 0$  and normalized boundary layer thickness  $\delta_{BL}/r_0$  varying from 0.025 up to 0.4 doubling the value of  $\delta_{BL}/r_0$  at each step. For clarity, the jet initial conditions are summarized in table 1.

$M$	$Re_D$	$TI$	$\delta/r_0$
0.9	$10^5$	0%	0.15
0.9	$10^5$	3%	0.15
0.9	$10^5$	6%	0.15
0.9	$10^5$	9%	0.15
0.9	$10^5$	12%	0.15
0.9	$10^5$	15%	0.15
0.9	$10^5$	0	0.025
0.9	$10^5$	0	0.05
0.9	$10^5$	0	0.1
0.9	$10^5$	0	0.2
0.9	$10^5$	0	0.4

**Table 1** Jet initial conditions

An in-house solver, based on the three-dimensional filtered compressible Navier–Stokes equations in cylindrical coordinates, has been used to perform the LES simulations. Specifically, the LESs were carried out using grids containing a number of points varying between 250 million and 1 billion, with low-dissipation schemes and relaxation filtering as a subgrid dissipation model [23].

More details on the LES can be found in references [24–26].

The present study is limited to the near-field domain, usually identified as the noise-producing region of the jet flow and thus of interest for jet-noise modelling. Pressure time series are extracted from virtual probes at different locations in the near field, covering a domain that spans from the nozzle exhaust up to  $x/D = 20$  in the axial direction and from the nozzle lip line ( $r/D = 0.5$ ) up to  $r/D = 3$  in the radial direction. The data set has been acquired at a sampling frequency corresponding to  $St=12.8$  for 3221-time snapshots.

### III. Post-Processing Procedure

The data processing relies on separating the acoustic component of the pressure signals from the hydrodynamic one. This goal is achieved by applying the procedure proposed by [20] and [21] that is briefly worked out in what follows.

The method is based on the wavelet transform of pressure signals and an appropriate filtering of the resulting wavelet coefficients. It is known that the wavelet transform performs well in identifying and isolating intermittent or time-dependent features. For a pressure time series  $p(t)$ , the wavelet transform can be formally represented by the following expression. [27–30]:

$$w(s, t) = C_{\psi}^{-\frac{1}{2}} s^{-\frac{1}{2}} \int_{-\infty}^{\infty} p(\tau) \psi^* \left( \frac{t - \tau}{s} \right) d\tau, \quad (1)$$

where  $s$  is the wavelet scale,  $\tau$  is a time shift,  $C_{\psi}^{-\frac{1}{2}}$  is a constant that takes into account the mean value of  $\psi(t)$  and  $\psi^* \left( \frac{t - \tau}{s} \right)$  is the complex conjugate of the dilated and translated mother wavelet  $\psi(t)$ .

With the aim of performing the acoustic/hydrodynamic separation, the wavelet coefficients can be separated by assuming that the hydrodynamic contribution, being related to localized eddy structures, compresses well onto the wavelet basis so that it originates, in the transformed domain, few but with large amplitude wavelet coefficients. Thus, the so-called pseudo-sound (i.e., the hydrodynamic component of pressure fluctuations) can be extracted by selecting the wavelet coefficients exceeding a proper threshold.

In the present approach, the threshold is identified through the so-called WT3 technique, presented in [21] and applied successfully also to other configurations out of jet noise (e.g. [31–33]). The method is based on single-point statistics thus it does not require additional signals taken from other microphones. The threshold is estimated through an iterative process originally developed for signal denoising [34] and then applied to the analysis of coherent structures in turbulence [35].

Once the wavelet coefficients are separated, the acoustic pressure is reconstructed in the time domain by the inverse transform of the wavelet coefficients having amplitude lower than the threshold and by setting to zero the other wavelet coefficients (i.e. those with amplitude larger than the threshold). Similarly, by setting to zero the coefficients with amplitude lower than the threshold, the hydrodynamic pressure can be recovered.

In summary, the procedure splits a given pressure signal into two time series representing the acoustic and the hydrodynamic pressure components. The two time series are then processed separately and relevant statistical properties are eventually computed.

An example in the Fourier domain of a decomposed signal is reported in figure 1 for  $x/D = 4$  and  $r/D = 1$ . It is shown that the hydrodynamic component contains most of the low-frequency energy content of the signal whereas the acoustic pressure is concentrated at higher frequencies. Further results obtained in the Fourier domain are presented in the next section.

### IV. Results

The results are firstly presented in terms of Overall Sound Pressure Level (*OASPL*), which is defined as follows:

$$OASPL = 20 \log_{10} \left( \frac{\sigma}{p_{\text{ref}}} \right), \quad (2)$$

where  $\sigma$  is the standard deviation of the pressure signal and  $p_{\text{ref}}$  is a reference pressure whose value is  $20 \mu Pa$ .

The *OASPL* spatial distributions for the different *TIs* are reported in figure 2. A strong directivity of the acoustic pressure towards the sideline ( $\approx 90^\circ$ , that corresponds to  $x/D$  close to 0) is observed for both the fully laminar and nominally laminar cases in figures 2 (a) and (b). This behaviour is likely ascribed to the fact that in the laminar case the noise generated by the small-scale coherent structures is more effective due to the formation and pairing of vortical structures near the nozzle exit. On the other hand, larger *TI* values induce the larger scales to be efficient noise sources and to dominate at larger  $x/D$ . Specifically, for increasing *TI* the directivity in the sideline direction is less pronounced

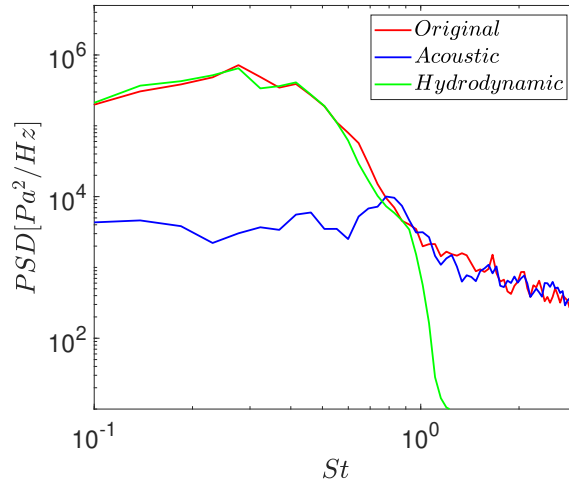


**Fig. 1** Decomposed pressure spectra, at  $x/D=4$  and  $r/D=1$ , for the jet with  $TI = 15\%$

and the noisiest region tends to extend downstream, reaching larger  $x/D$  distances. For turbulence levels larger than 10% (see cases 2 (e) and (f)), the influence of  $TI$  on the acoustic near field becomes less significant.

Figure 3 reports the OASPL of the acoustic pressure for different boundary layer thicknesses. It is observed that the BL thickness does not affect significantly the sideline directivity whereas it influence significantly its intensity. For increasing  $\delta/r_0$ , the OASPL in the sideline direction slightly deviates towards larger angles. This effect might be related to a retarded destabilization of the vortices generated by the roll up of the shear layer. Indeed, the Kelvin-Helmholtz (K-H) instability waves tends to destabilize at larger  $x/D$  for increasing  $\delta/r_0$ .

On the other hand, for increasing BL thickness, the high amplitude OASPL region close to the jet axis tends to be more concentrated and to have a smaller extension in terms of  $x/D$ . As an example, at the lowest  $\delta/r_0$  (case 3 a) OASPL of the order of 155dB is observed up to  $x/D$  of about 15. At the largest thickness (case case 3 e), this OASPL amplitude is reached at  $x/D$  about 10. This result suggests that a large BL thickness on one side retards the destabilization of the K-H waves but on the other side leads a more rapid transition to turbulence of the shear layer. Therefore, the extension of the noise producing region decreases for increasing  $\delta/r_0$ .

The frequency dependence of the Fourier energy is determined through the acoustic spectra estimated in terms of the Sound Pressure Level (SPL) which is given by following equation:

$$SPL = 10 \log_{10} \left( \frac{PSD \Delta f_{ref}}{p_{ref}^2} \right), \quad (3)$$

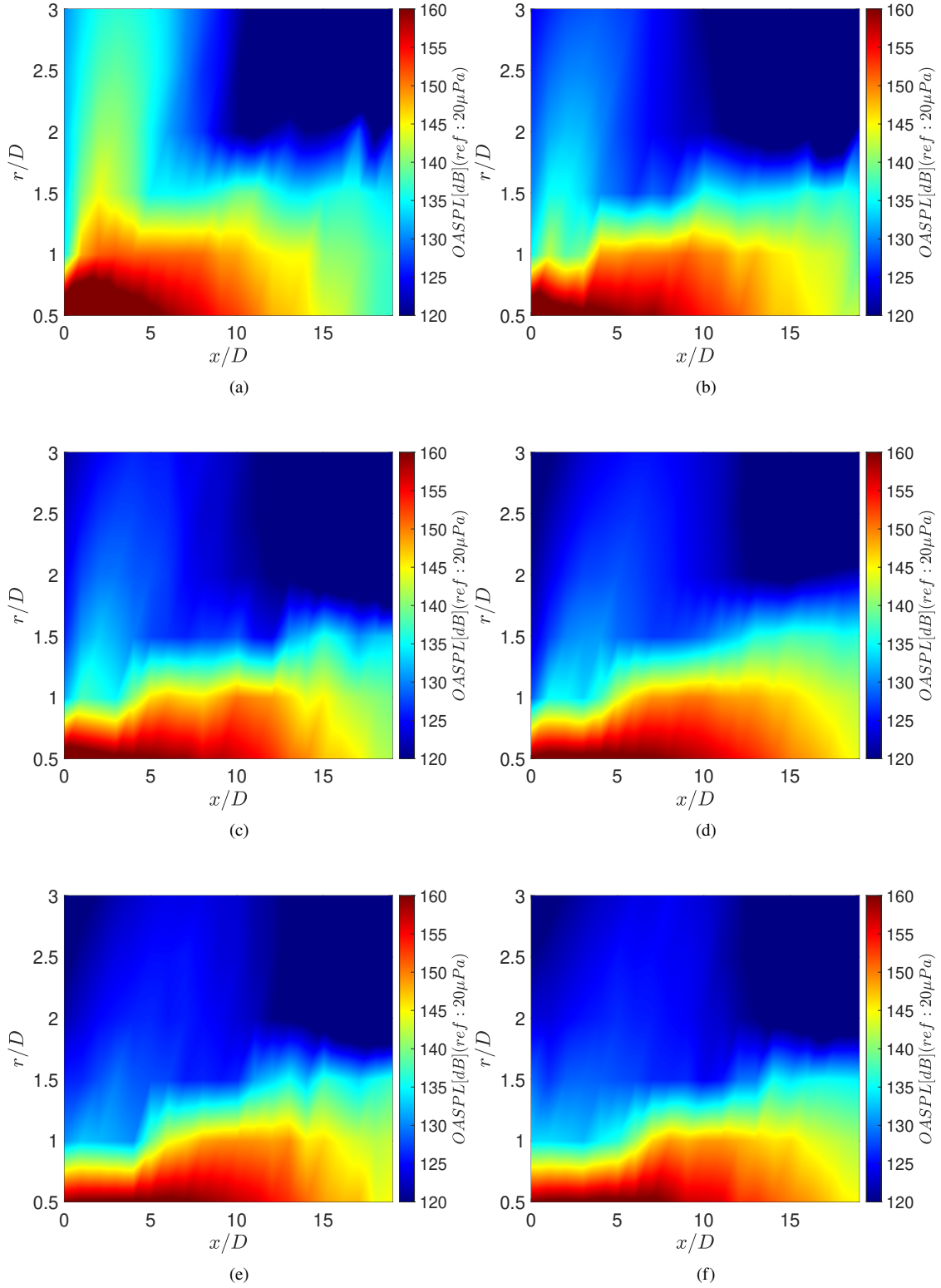
where PSD denotes the power spectral density evaluated using the Welch's method. For the sake of conciseness, results have been reported only for two representative radial locations.

Figure 4 presents the near-field acoustic spectra for different Turbulence Intensities, two radial positions and different  $x/D$ . Results for different BL thicknesses are presented in figure 5. Figure 4 shows that  $TI$  substantially affects the near-field acoustic pressure only when the nozzle exhaust flow is laminar or transitional. As expected, the modification of the spectra shape due to this parameter is more evident at axial locations of about  $x/D \leq 10$ .

As shown in figure 5, the increase in the thickness of the boundary layer causes, at low axial distances, an increase in the intensity of the acoustic field over approximately the entire frequencies range analysed. It is worth noting that, at  $x/D = 0.5$  (figures 5 (a) and (b))  $\delta_{BL} = 0.2$  seems to be a transitional point, indeed for values higher than it, the energy content of the spectra is observed to decrease with a simultaneous appearance of peaks at  $St \approx 0.3$ . As the axial distance increases, the effect of the boundary layer thickness becomes negligible.

## V. Conclusions

The present paper reports an analysis of the influence of the nozzle exit condition of a compressible subsonic jet on the near-field acoustic pressure. The investigation is performed by processing a numerical database obtained by



**Fig. 2 OASPL acoustic maps for different nozzle exhaust turbulence intensities: a) TI=0%; b)TI=3%; c)TI=6%; d)TI=9%; e)TI=12%, f)TI=15%.**

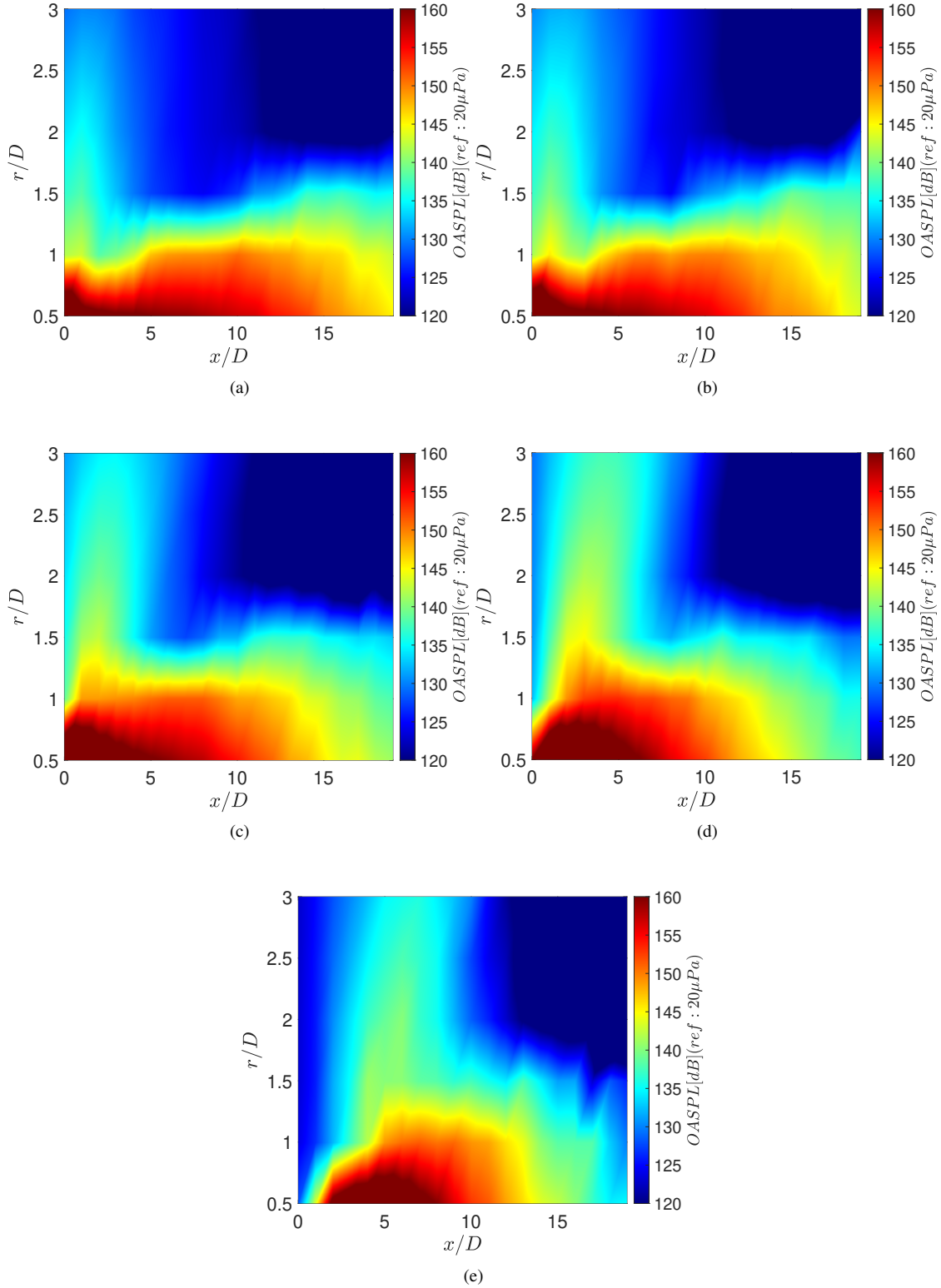


**Fig. 3** OASPL acoustic maps for different nozzle exhaust boundary layer thicknesses: a)  $\delta/r_0 = 0.025$ ; b)  $\delta/r_0 = 0.05$ ; c)  $\delta/r_0 = 0.1$ ; d)  $\delta/r_0 = 0.2$ ; e)  $\delta/r_0 = 0.4$ .

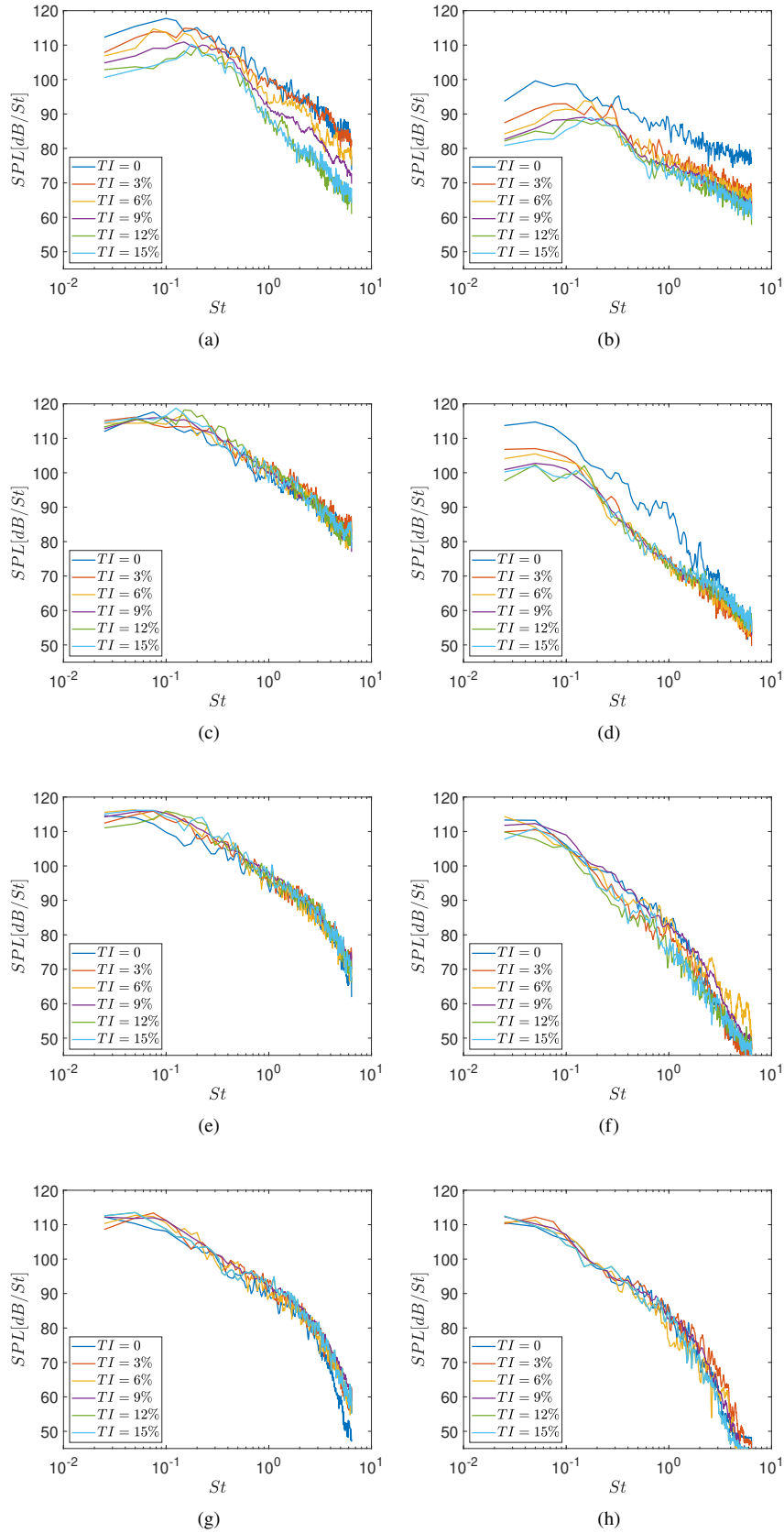


**Fig. 4** SPLs spectra for different turbulence intensities at: a)  $x/D=5$  and  $r/D=1$ ; b)  $x/D=5$  and  $r/D=2$ ; c)  $x/D=10$  and  $r/D=1$ ; d)  $x/D=10$  and  $r/D=2$ ; e)  $x/D=15$  and  $r/D=1$ ; f)  $x/D=15$  and  $r/D=2$ ; g)  $x/D=20$  and  $r/D=1$ ; h)  $x/D=20$  and  $r/D=2$ ;

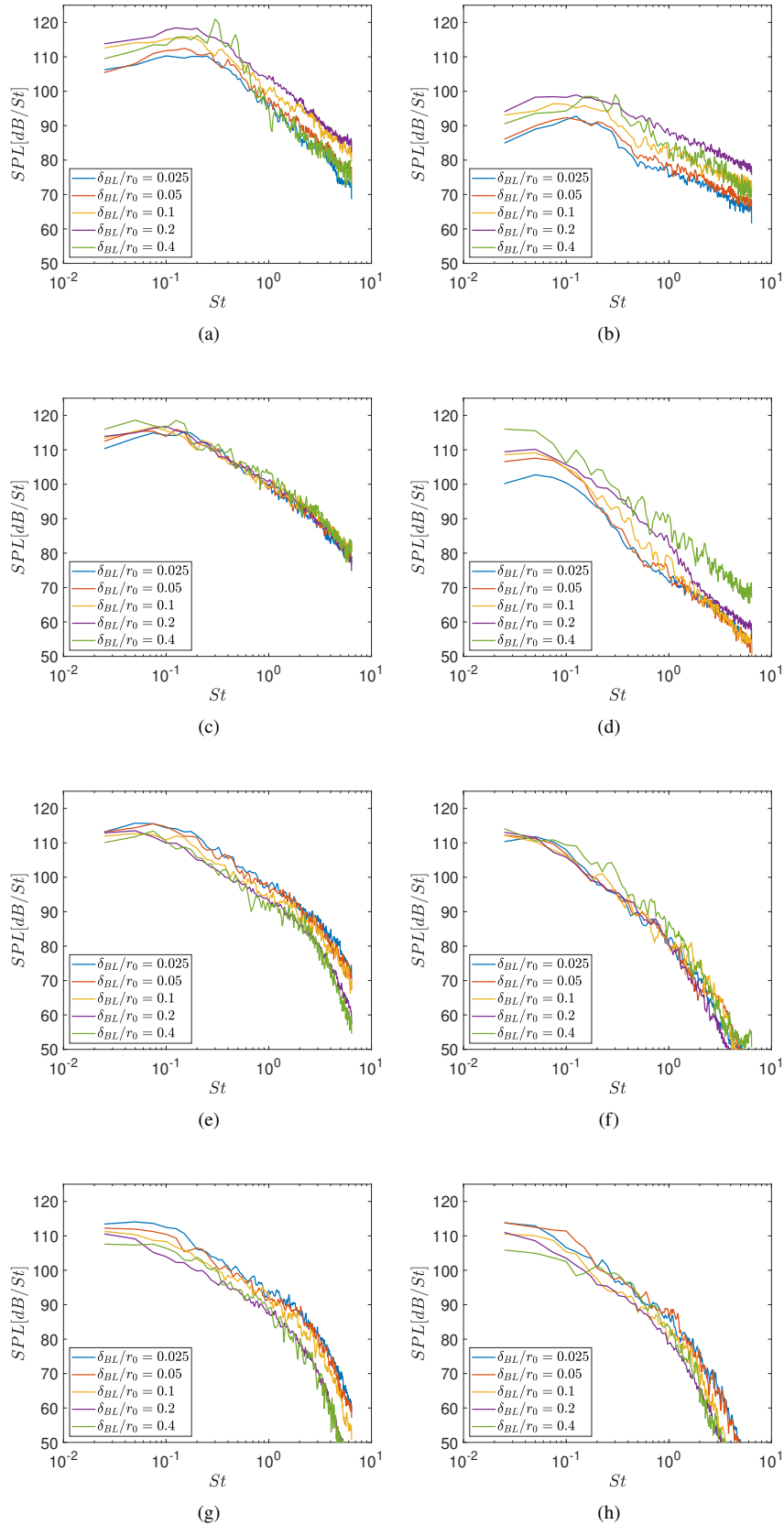


Fig. 5 SPLs spectra for different boundary layer thicknesses at: a)  $x/D=5$  and  $r/D=1$ ; b)  $x/D=5$  and  $r/D=2$ ; c)  $x/D=10$  and  $r/D=1$ ; d)  $x/D=10$  and  $r/D=2$ ; e)  $x/D=15$  and  $r/D=1$ ; f)  $x/D=15$  and  $r/D=2$ ; g)  $x/D=20$  and  $r/D=1$ ; h)  $x/D=20$  and  $r/D=2$ ;

well-resolved LES at fixed Mach and Reynolds numbers. The different TIs are obtained at constant boundary layer thickness, whereas the cases with different boundary layer thicknesses corresponds to laminar conditions. The acoustic pressure component is extracted from the pressure time series by the application of an existing wavelet-based procedure that relies on the application of an iterative process which converges rapidly. The acoustic pressure at low TIs showed a relevant OASPL in the sideline direction. The intensity reduces by increasing the TI and disappears when the jet is fully developed. The OASPL is strongly influenced by the boundary layer thickness in the laminar case. Specifically, as the boundary layer thickens, the sideline signature moves downstream and increases in intensity whereas the extension of the high OASPL region in terms of  $x/D$  reduces significantly for increasing thickness. The acoustic spectra, presented in terms of SPL, are slightly influenced by the turbulence intensity both for what concerns their shape and their magnitude. Specifically, it is observed an increase of noise at the mid-high frequencies, especially at lower  $x/D$ , for decreasing TI. On the other hand, the BL thickness does not seem to influence the spectra shape but induces a variation of the overall energy content.

Further analyses are surely needed to better quantify the influence of the jet exit parameters and to develop suited models able to predict their effect on the OASPL and the Fourier spectra. These challenging tasks will be pursued in the near future.

### Acknowledgments

C. Bogey was partially supported by the LABEX CeLyA (ANR-10-LABX-0060/ANR-16-IDEX-0005).

The numerical data analyzed in this work were obtained using the HPC resources of PMCS2I (Pôle de Modélisation et de Calcul en Sciences de l'Ingénieur et de l'Information) of Ecole Centrale de Lyon and P2CHPD (Pôle de Calcul Hautes Performances Dédié) of Université Lyon I, and the resources of CINES (Centre Informatique National de l'Enseignement Supérieur) and IDRIS (Institut du Développement et des Ressources en Informatique Scientifique) under the allocation 2021-2a0204 made by GENCI (Grand Equipement National de Calcul Intensif).

### References

- [1] Lighthill, M. J., "On sound generated aerodynamically," *General theory. Proc. R. Soc. Lond.*, 1952, pp. 564–587.
- [2] Goldstein, M. E., "Aeroacoustics of turbulent shear flows," *Annu. Rev. Fluid Mech.*, Vol. 16, No. 1, 1984, pp. 263–285.
- [3] Lilley, G., "On the noise from air jets." *AGARD CP 131*, 1974, pp. 13.1–13.2.
- [4] Cavalieri, A. V. G., Jordan, P., Agarwal, A., and Gervais, Y., "Jittering wave-packet models for subsonic jet noise," *J. Sound Vib.*, Vol. 330, No. 18-19, 2011, pp. 4474–4492.
- [5] Jordan, P., and Colonius, T., "Wave packets and turbulent jet noise," *Annu. Rev. Fluid Mech.*, Vol. 45, No. 1, 2013, pp. 173–195.
- [6] Cavalieri, A. V. G., Jordan, P., and Lesshafft, L., "Wave-packet models for jet dynamics and sound radiation," *Appl. Mech. Rev.*, Vol. 71, No. 2, 2019.
- [7] Palma, G., Meloni, S., Camussi, R., Iemma, U., and Bogey, C., "Data-Driven Multiobjective Optimization of Wave-Packets for Near-Field Subsonic Jet Noise," *AIAA Journal*, Vol. 0, No. 0, 0, pp. 1–9. <https://doi.org/10.2514/1.J062261>.
- [8] Gutmark, E., and Ho, C. M., "Preferred modes and the spreading rates of jets," *The Physics of Fluids*, Vol. 26, No. 10, 1983, pp. 2932–2938.
- [9] Crighton, D. G., "Acoustics as a branch of fluid mechanics," *Journal of Fluid Mechanics*, Vol. 106, 1981, pp. 261–298.
- [10] Bogey, C., and Sabatini, R., "Effects of nozzle-exit boundary-layer profile on the initial shear-layer instability, flow field and noise of subsonic jets," *Journal of Fluid Mechanics*, Vol. 876, 2019, p. 288–325. <https://doi.org/10.1017/jfm.2019.546>.
- [11] Bogey, C., and Marsden, O., "Identification of the effects of the nozzle-exit boundary-layer thickness and its corresponding Reynolds number in initially highly disturbed subsonic jets," *Physics of Fluids*, Vol. 25, No. 5, 2013. <https://doi.org/10.1063/1.4807071>.
- [12] Ho, C., and Huerre, P., "Perturbed Free Shear Layers," *Annual Review of Fluid Mechanics*, Vol. 16, No. 1, 1984, pp. 365–422. <https://doi.org/10.1146/annurev.fl.16.010184.002053>, URL <https://doi.org/10.1146/annurev.fl.16.010184.002053>.
- [13] Bogey, C., "Generation of Excess Noise by Jets with Highly Disturbed Laminar Boundary-Layer Profiles," *AIAA Journal*, Vol. 59, No. 2, 2021, pp. 569–579. <https://doi.org/10.2514/1.J059610>, URL <https://doi.org/10.2514/1.J059610>.

- [14] Zaman, K. B. M. Q., “Increased Jet Noise Due to a “Nominally Laminar” State of Nozzle Exit Boundary Layer,” *NASA report*, 2017.
- [15] Bogey, C., and Bailly, C., “Influence of nozzle-exit boundary-layer conditions on the flow and acoustic fields of initially laminar jets,” *Journal of Fluid Mechanics*, Vol. 663, 2010, pp. 507–538.
- [16] Bogey, C., Marsden, O., and Bailly, C., “Influence of initial turbulence level on the flow and sound fields of a subsonic jet at a diameter-based Reynolds number of  $10^5$ ,” *Journal of Fluid Mechanics*, Vol. 701, 2012, p. 352–385. <https://doi.org/10.1017/jfm.2012.162>.
- [17] Tinney, C. E., and Jordan, P., “The near pressure field of co-axial subsonic jets,” *Journal of Fluid Mechanics*, Vol. 611, 2008, p. 175–204. <https://doi.org/10.1017/S0022112008001833>.
- [18] Guj, G., and Camussi, R., “Statistical analysis of local turbulent energy fluctuations,” *Journal of Fluid Mechanics*, Vol. 382, 1999, p. 1–26. <https://doi.org/10.1017/S0022112098003553>.
- [19] Arndt, R. E. A., Long, D. F., and Glauser, M. N., “The proper orthogonal decomposition of pressure fluctuations surrounding a turbulent jet,” *Journal of Fluid Mechanics*, Vol. 340, 1997, p. 1–33. <https://doi.org/10.1017/S0022112097005089>.
- [20] Grizzi, S., and Camussi, R., “Wavelet analysis of near-field pressure fluctuations generated by a subsonic jet,” *Journal of Fluid Mechanics*, Vol. 698, 2012, pp. 93–124.
- [21] Mancinelli, M., Pagliaroli, T., Di Marco, A., Camussi, R., and Castelain, T., “Wavelet decomposition of hydrodynamic and acoustic pressures in the near field of the jet,” *Journal of Fluid Mechanics*, Vol. 813, 2017, pp. 716–749.
- [22] Mancinelli, M., Pagliaroli, T., Camussi, R., and Castelain, T., “On the hydrodynamic and acoustic nature of pressure proper orthogonal decomposition modes in the near field of a compressible jet,” *J. Fluid Mech.*, Vol. 836, 2018, pp. 998–1008.
- [23] Bogey, C., Marsden, O., and Bailly, C., “Large-eddy simulation of the flow and acoustic fields of a Reynolds number  $10^5$  subsonic jet with tripped exit boundary layers,” *Physics of Fluids*, Vol. 23, 2011, p. 035104.
- [24] Bogey, C., “Acoustic tones in the near-nozzle region of jets: characteristics and variations between Mach numbers 0.5 and 2,” *Journal of Fluid Mechanics*, Vol. 921, 2021. <https://doi.org/10.1017/jfm.2021.426>.
- [25] Bogey, C., “Grid sensitivity of flow field and noise of high-Reynolds-number jets computed by large-eddy simulation,” *International Journal of Aeroacoustics*, Vol. 17, No. 4-5, 2018, pp. 399–424. <https://doi.org/10.1177/1475472X18778287>, URL <https://doi.org/10.1177/1475472X18778287>.
- [26] Bogey, C., “A database of flow and near pressure field signals obtained for subsonic and nearly ideally expanded supersonic free jets using large-eddy simulations,” <https://hal.archives-ouvertes.fr/hal-03626787>, 2022.
- [27] Farge, M., “Wavelet transform and their applications to turbulence,” *Annual Review of Fluid Mechanics*, Vol. 24, No. 1, 1992, pp. 395–458. <https://doi.org/10.1146/annurev.fl.24.010192.002143>.
- [28] Camussi, R., Robert, G., and Jacob, M. C., “Cross-wavelet analysis of wall pressure fluctuations beneath incompressible turbulent boundary layers,” *Journal of Fluid Mechanics*, Vol. 617, 2008, p. 11–30. <https://doi.org/10.1017/S002211200800373X>.
- [29] Meloni, S., Lawrence, J. L., Proença, A. R., Self, R. H., and Camussi, R., “Wall pressure fluctuations induced by a single stream jet over a semi-finite plate,” *International Journal of Aeroacoustics*, Vol. 19, No. 3-5, 2020, pp. 240–253. <https://doi.org/10.1177/1475472X20930650>, URL <https://doi.org/10.1177/1475472X20930650>.
- [30] Micci, G. L., Camussi, R., Meloni, S., and Bogey, C., “Intermittency and Stochastic Modeling of Low- and High-Reynolds-Number Compressible Jets,” *AIAA Journal*, Vol. 60, No. 3, 2022, pp. 1983–1990. <https://doi.org/10.2514/1.J061128>, URL <https://doi.org/10.2514/1.J061128>.
- [31] Li, S., Rival, D. E., and Wu, X., “Sound source and pseudo-sound in the near field of a circular cylinder in subsonic conditions,” *Journal of Fluid Mechanics*, Vol. 919, 2021, p. A43. <https://doi.org/10.1017/jfm.2021.404>.
- [32] Hajczak, A., Sanders, L., Vuillot, F., and Druault, P., “Wavelet-Based Separation Methods Assessment on the Near Pressure Field of a Landing Gear Subcomponent,” *25th AIAA/CEAS Aeroacoustics Conference*, 2019, p. 2482. <https://doi.org/10.2514/6.2019-2482>.
- [33] Pérez Arroyo, C., Daviller, G., Puigt, G., Airiau, C., and Moreau, S., “Identification of temporal and spatial signatures of broadband shock-associated noise,” *Shock Waves*, Vol. 29, No. 1, 2019, pp. 117–134. <https://doi.org/10.1007/s00193-018-0806-4>.

- [34] Donoho, D. L., and Johnstone, J. M., “Ideal spatial adaptation by wavelet shrinkage,” *Biometrika*, Vol. 81, No. 3, 1994, pp. 425–455.
- [35] Ruppert-Felsot, J., Farge, M., and Petitjeans, P., “Wavelet tools to study intermittency: application to vortex bursting,” *J. Fluid Mech.*, Vol. 636, 2009, pp. 427–453.